Supporting Information

Magnetic Graphene Quantum Facilitate Dots Closed-Tube One-Step Detection of SARS-CoV-2 with Ultra-Low Field Nuclear Magnetic Resonance

Yongqiang Li [a, c, e, f, 1], *Peixiang Ma* [b, 1], *Quan Tao* [a, c, e, f], *Hans-Joachim Krause* [d, e], *Siwei Yang* [a, e, f, *], *Guqiao Ding* [a, f, *], *Hui Dong* [a, c, e, f, *], *and Xiaoming Xie* [a, c, e, f]

[a] State Key Laboratory of Functional Materials of Informatics, Shanghai Institute of Microsystem and Information Technology (SIMIT), Chinese Academy of Sciences, Shanghai 200050, P. R. China.
[b] Shanghai Institute for Advanced Immunological Studies, ShanghaiTech University, Shanghai 201210, P. R. China.
[c] CAS Center for ExcelleNce in Superconducting Electronics (CENSE), Chinese Academy of Sciences, Shanghai 200050, P. R. China.
[d] Institute of Biological Information Processing (IBI-3), Forschungszentrum Jülich (FZJ), D-52425 Jülich, Germany.
[e] Joint Research Institute on Functional Materials and Electronics, Collaboration between SIMIT and FZJ.
[f] Center of Materials Science and Optoelectronics Engineering, University of Chinese Academy of Sciences (UCAS), Beijing 100049, P. R. China.

[1] These authors contributed equally.
* Siwei Yang - E-mail: yangsiwei@mail.sim.ac.cn; * Guqiao Ding - E-mail: gqding@mail.sim.ac.cn; * Hui Dong - E-mail: donghui@mail.sim.ac.cn

Supplementary Figures

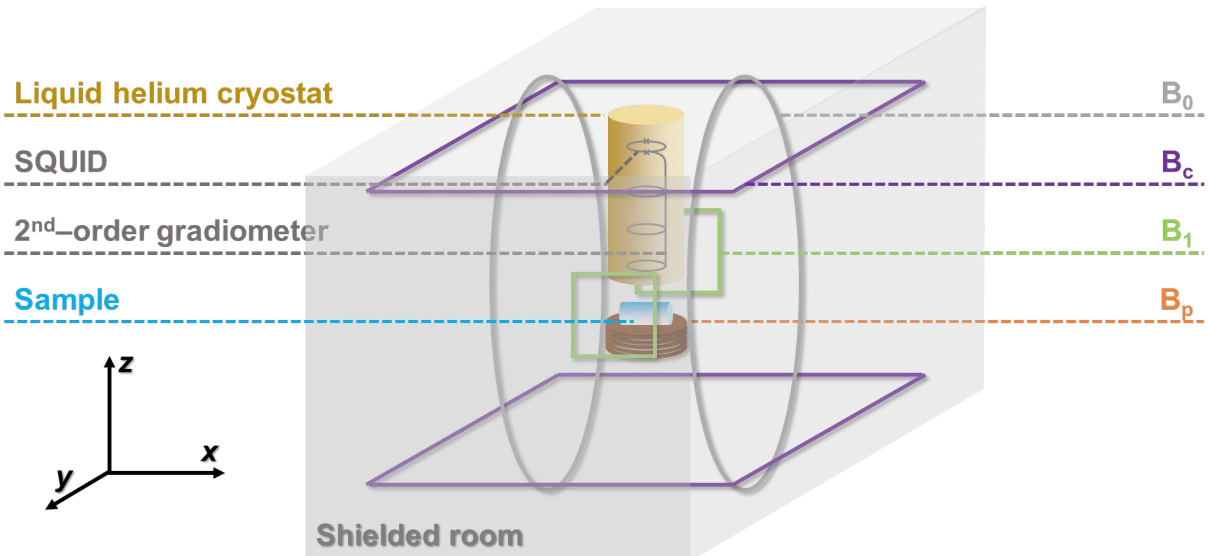

Fig. S1. Depiction of the homemade ULF NMR system.

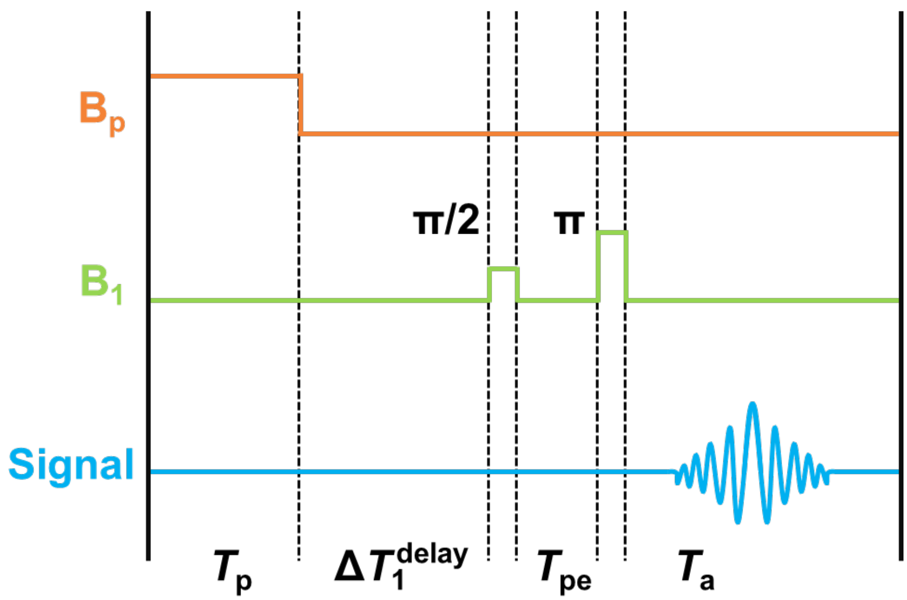

Fig. S2. Pulse sequence for T_1 measurement in ULF NMR system.

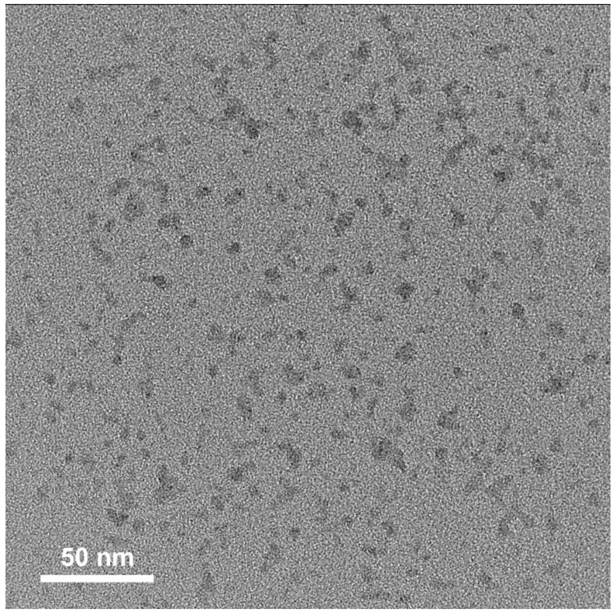

Fig. S3. Transmission electron microscopy (TEM) image of GQDs. The image shows that GQDs have a great dispersity, which is proven by the zeta potential measurement (–46.2 mV).

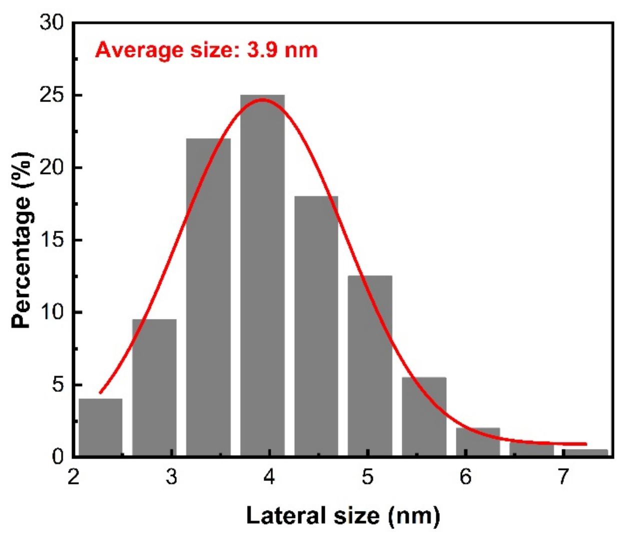

Fig. S4. Size distribution histogram of GQDs derived from **Fig. S3**. A Gaussian distribution fit was used to analyse the average size of GQDs. The average size of GQDs is found to be 3.9 nm.

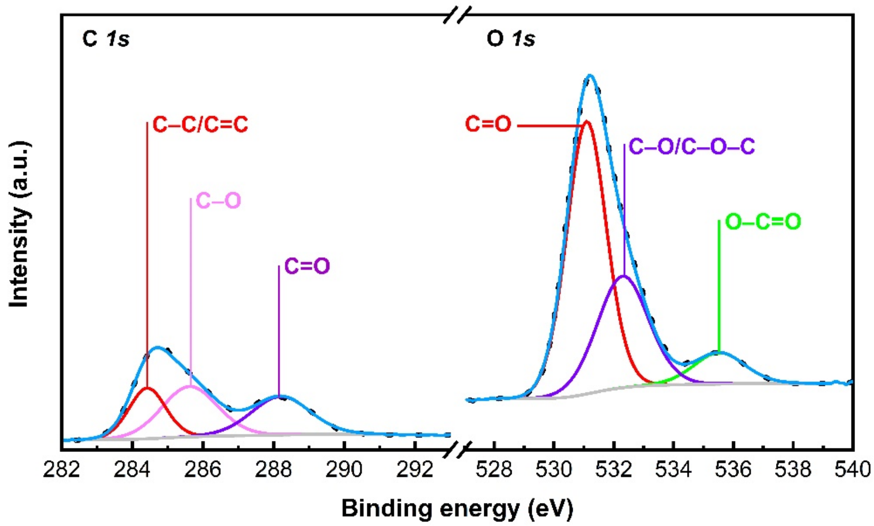

Fig. S5. High-resolution X-ray photoelectron spectroscopy (XPS) C *1s* and O *1s* spectra of GQDs. In the C *1s* spectrum of GQDs, peaks located at 284.4, 285.6, and 288.2 eV are recognized as C–C/C=C, C–O, and C=O bonds, respectively, while the peaks located at 531.1, 532.3, and 535.5 eV in the O *1s* spectrum can be attributed to C=O, C–O/C–O–C, and O–C=O bonds, respectively.

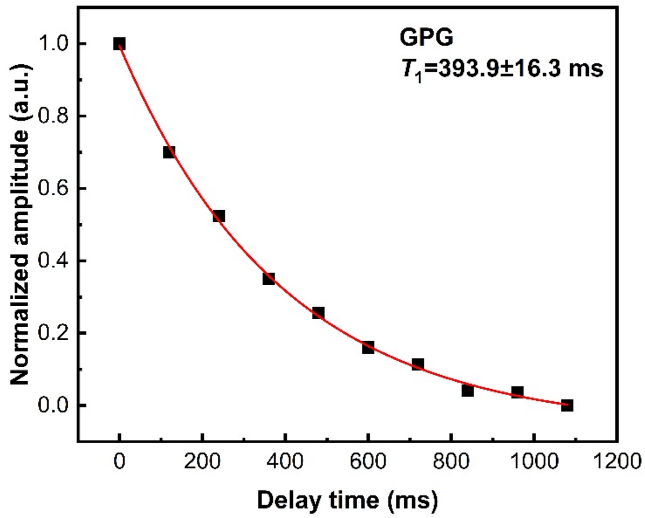

Fig. S6. T_1 fitting of GPG in PBS buffer.

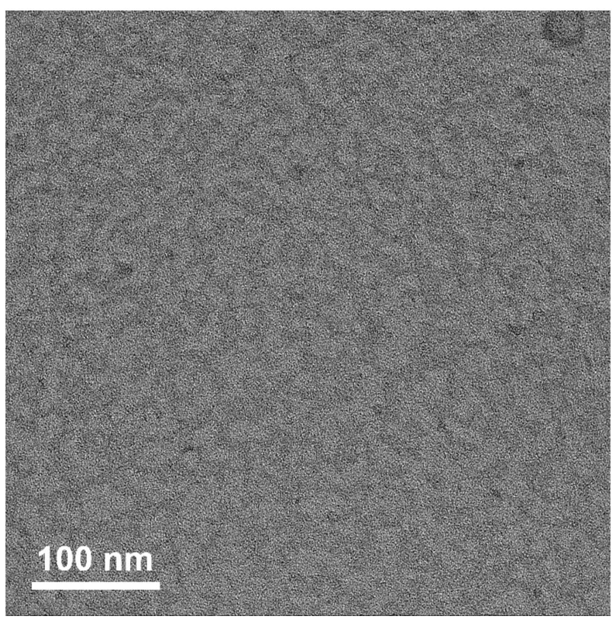

Fig. S7. TEM image of GPG-Abs. The scale bar is 100 nm in the image.

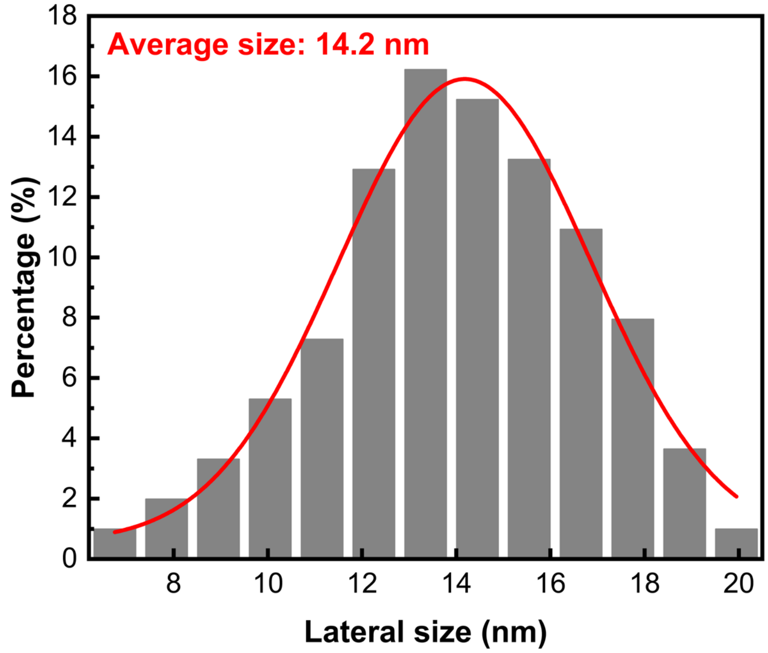

Fig. S8. Size distribution histogram of GPG-Abs. The average lateral size of GPG-Abs is 14.2 nm, which is larger than that of GPG.

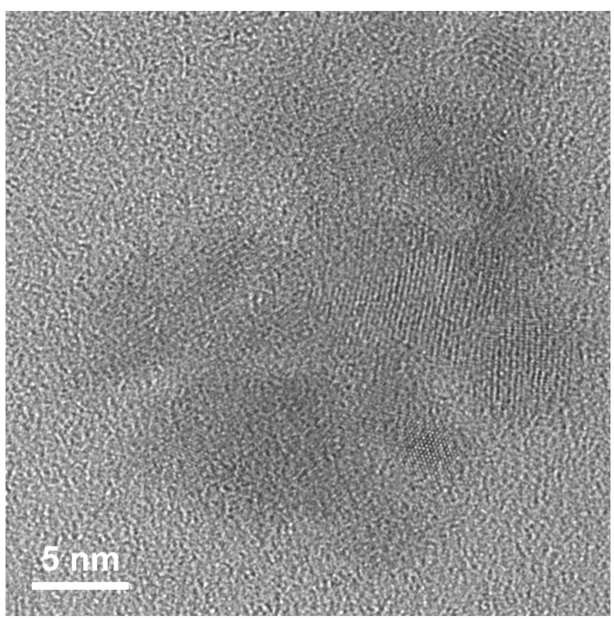

Fig. S9. HR-TEM image of GPG-Abs. The scale bar is 5 nm in the image. GPG can be recognized as the assembly after the conjugation with Abs.

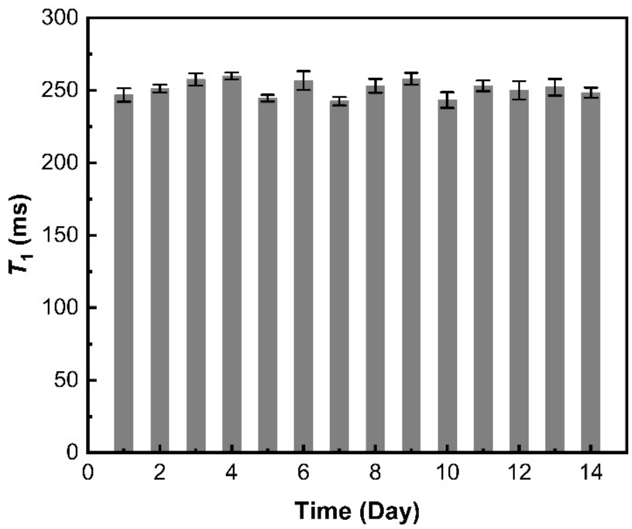

Fig. S10. Stability of GPG-Abs. T_1s of GPG-Ab measured at different times after the preparation.

Supplementary Table

Table S1. Comparison of newly developed methods for SARS-CoV-2 detection. [a)]

Method	Targeting molecule	Pretreat-ment	Direct virus detection	Detection time	LOD	Ref.
MRSw	S protein	No	Yes	2 min	248 Particles mL^{-1}	This work
Colorimetry	RNA	Yes	No	10 min	0.18 ng μL^{-1}	[1]
FET	S protein	No	Yes	few min	242 copies mL^{-1}	[2]
LSPR	RNA	Yes	No	10 min	0.22 pM	[3]
CRISPR	RNA	Yes	No	20 min	4.6 copies	[4]
LAMP	RNA	Yes	No	30–90 min	42 copies/reaction	[5]

[a)] Abbreviations in this table: LOD, limit of detection; MRSw: magnetic relaxation switches; FET, field-effect transistor; LSPR, localized surface plasmon resonance; CRISPR, clustered regularly interspaced short palindromic repeats; LAMP, loop-mediated isothermal amplification.

Table S2. The detailed costs of GPG preparation for a single test.

Category	Item	Usage	Price per unit	Cost
	$Gd(NO_3)_3$	0.1 μmol	USD 2/mmol	USD 0.0002
Material	PEG_6	0.01 mmol	USD 10/mmol	USD 0.1
	GQDs	1.5 mg	USD 300/g	USD 0.45
Power	Electricity	6 kW·h[a)]	USD 0.1/kW·h	USD 0.6
Storage	Vial	1	USD 0.1	USD 0.1
		Total cost		**USD 1.2502**

[a)] In this work, about 300 kW·h of electricity is consumed for an entire process of hydrothermal reaction. Practically, 50 portions of the probe can be synthesized at one time, so the electricity used for synthesis is 6 kW·h per portion of the probe.

Supplementary References

[1] P. Moitra, M. Alafeef, K. Dighe, M.B. Frieman, D. Pan, Selective Naked-Eye Detection of SARS-CoV-2 Mediated by N Gene Targeted Antisense Oligonucleotide Capped Plasmonic Nanoparticles, ACS Nano, 14(2020) 7617-27.
[2] G. Seo, G. Lee, M.J. Kim, S.H. Baek, M. Choi, K.B. Ku, et al., Rapid Detection of COVID-19 Causative Virus (SARS-CoV-2) in Human Nasopharyngeal Swab Specimens Using Field-Effect Transistor-Based Biosensor, ACS Nano, 14(2020) 5135-42.
[3] G.G. Qiu, Z.B. Gai, Y.L. Tao, J. Schmitt, G.A. Kullak-Ublick, J. Wang, Dual-Functional Plasmonic Photothermal Biosensors for Highly Accurate Severe Acute Respiratory Syndrome Coronavirus 2 Detection, ACS Nano, 14(2020) 5268-77.
[4] X. Ding, K. Yin, Z.Y. Li, R.V. Lalla, E. Ballesteros, M.M. Sfeir, et al., Ultrasensitive and Visual Detection of SARS-CoV-2 Using All-in-One Dual CRISPR-Cas12a Assay, Nat. Commun., 11(2020) 4711.
[5] F.W.N. Chow, T.T.Y. Chan, A.R. Tam, S.H. Zhao, W.M. Yao, J. Fung, et al., A Rapid, Simple, Inexpensive, and Mobile Colorimetric Assay COVID-19-LAMP for Mass On-Site Screening of COVID-19, Int. J. Mol. Sci., 21(2020) 5380.